

DETECTION OF ASR DAMAGE IN CONCRETE USING CONTACTLESS ULTRASONIC SCANNING

John S. Popovics¹

Dept. Civil and Environmental Engineering
University of Illinois at Urbana-Champaign
Urbana, IL

Homin Song

Nuclear Science and Engineering Division
Argonne National Laboratory
Lemont, IL

ABSTRACT

Here we investigate the use of contactless ultrasonic surface wave measurements to detect and characterize ASR-induced cracking damage in concrete. Observations from laboratory tests and a study on ASR concrete samples in a controlled testbed reveal that ultrasonic surface wave backscatter measurements can be used to detect and locate distributed cracking in concrete. Sub-wavelength imaging is achieved by isolating the backscatter owing to cracking from that owing to natural material homogeneity (aggregates) in the concrete through the use of a frequency-wavenumber domain analysis approach.

Keywords: alkali-silica reactivity, cracking, imaging, scatter.

1. INTRODUCTION

Concrete is a critical construction material for important infrastructure systems such as bridges and nuclear power plants. During its service life, concrete structures are subject to various deterioration mechanisms including freezing/thawing cycles, alkali-silica reaction (ASR) and sulfate attack [1-2]. Prolonged and repeated exposure to the mechanisms can lead to the initiation of damage to structures, and the damage grows during the remaining service life of the concrete structures unless appropriately repaired. To repair and retrofit damaged structures effectively, material damage needs to be detected and characterized early on in the process. Among various deterioration mechanisms, ASR is the specific mechanism of interest in this study. Although existing nondestructive evaluation (NDE) approaches have shown the potential, detecting and characterizing damage in concrete are still challenging tasks mainly because of natural heterogeneity and material variability of the concrete itself [3-4].

In this study, a new effective NDE technique is developed based on contactless ultrasonic scanning measurements to detect and characterize possible ASR damage in concrete. To do so, a contactless ultrasonic wavefield imaging

hardware and a wavefield data processing method are developed. The developed wavefield imaging hardware consists of a multi-channel MEMS ultrasonic microphone array with a signal conditioning circuit to enable rapid ultrasonic wavefield data acquisition with high a signal-to-noise ratio (SNR) and an automated mechanical scanner for efficient array scanning and positioning. Then, the wavefield data processing technique is developed based on a solid understanding of the interaction between incident ultrasonic waves and distributed sub-wavelength cracks through analytical studies, a series of numerical simulations and laboratory-scale experiments. The developed NDE technique is then applied to large-scale concrete block samples under realistic ASR environments. The experimental results demonstrate that the developed contactless wavefield imaging hardware enables rapid acquisition of high-quality ultrasonic wavefield data and that the proposed wavefield data processing technique successfully detects and characterizes ASR damage in concrete.

2. METHOD AND TESTS

2.1 Contactless ultrasonic measurements

The ultrasonic data are collected using scanning hardware designed and constructed by the second author. A photo of the data collection equipment is shown in Fig. 1. The ultrasonic data were collected at 120 x 8 scanning positions where the sending transducer was fixed in space and the receiving transducer array was moved at 2.5 mm-increments for a total of 960 measured signals. Once ultrasonic wavefield data were collected from each concrete sample, a frequency-wavenumber (f-k) processing technique was applied to extract incoherent scattering energy and detect and characterized ASR damage present in the tested concrete samples. The process involves the application of forward and inverse Fourier transforms (FT) carried out by considering a 3-D data structure of the collected wavefield data (one dimension in time t and two more dimensions in space x, y). The procedure is summarized below as a series of steps. In

¹ Contact author: johnpop@illinois.edu

Step 1 of the process, a 3-D FT is applied to convert the wavefield data from time-space (t-x-y) to frequency-wavenumber (f-kx-ky) domains. In Step 2, the transform is decomposed into incoherent scattering and coherent forward propagating wave field components by multiplying f-k domain filtering masks. In Step 3, the two decomposed wavefield components are then converted back into time-space domain using an inverse 3-D FT. In Step 4, the time-cumulative signal energies are computed up to time of signal duration for both wavefield components. Finally the normalized scattering energy is computed.

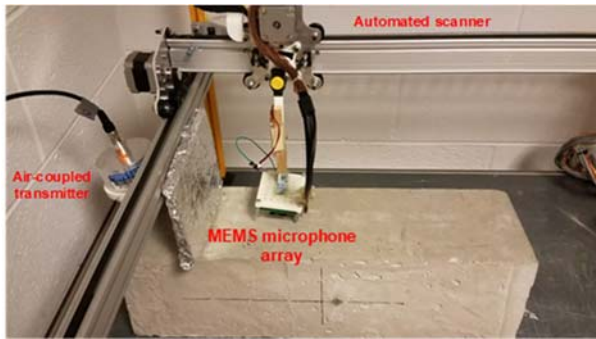


FIGURE 1: TESTING SETUP FOR CONTACTLESS ULTRASONIC SURFACE WAVE MEASUREMENTS ON CONCRETE. THE POSITION OF THE AIR-COUPLED SENDING TRANSDUCER IS FIXED, WHILE THE RECEIVER ARRAY MOVES AT SMALL INCREMENTS TO COLLECT SCAN DATA.

2.2 NIST ASR TEST BED

Four large-scale concrete samples with different levels of ASR-reactivity were prepared at the NIST testbed at their laboratory. The control sample (Mixture 4) includes low-alkali cement (<0.60 % Na₂O_{eq}) and non-reactive aggregate, while Reactive samples 1 to 3 (Mixtures 1 to 3) contain high-alkali cement (0.80 % Na₂O_{eq}) and reactive aggregate with different levels of alkali-silica reactivity. Laboratory tests carried out by NIST on small-scale companion samples showed that Mixtures 1 to 3 are potentially susceptible to ASR damage with different degrees while Mixture 4 is not. The four tested concrete samples are seen in Fig. 2. All the samples have the same dimensions (4.88 m × 1.83 m × 1.07 m) and steel reinforcement placement scheme.

3. RESULTS AND DISCUSSION

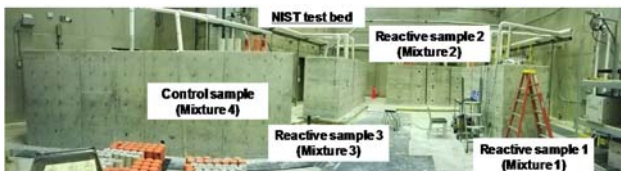


FIGURE 2: REINFORCED CONCRETE BLOCK SAMPLE TEST BED AT NIST. ULTRASONIC TESTS WERE CONDUCTED ON THE TOP SURFACES OF THE SAMPLES.

Figure 3 shows normalized incoherent scattering energy maps, computed from the data collected for the sample cases 6 months after sample casting. These results show good agreement with those from a numerical simulation and laboratory-scale experimental results that the authors also carried out. The reactive samples show higher scattered wave energy values while the control sample exhibits negligible scattered wave energy values throughout the scanned area. These experimental results demonstrate the feasibility potential of the proposed wavefield imaging hardware and the wavefield data processing approach to detect and locate ASR damage. However, the obtained results must be compared to other more direct measurements of ASR activity in the blocks to confirm actual ASR expansion within the samples.

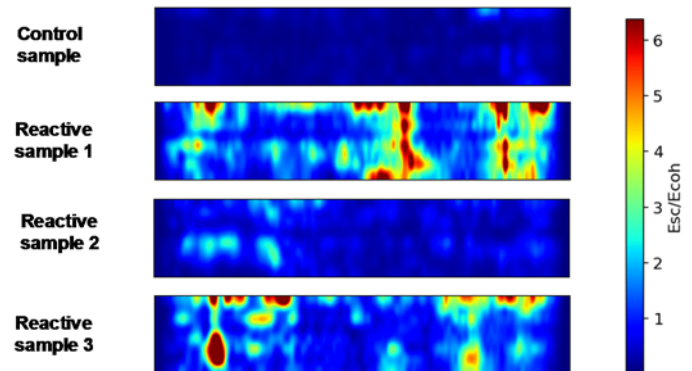


Figure 3: SCATTERED WAVE ENERGY MAP DATA OVER A CONSISTENT SCAN FOOTPRINT ON EACH BLOCK SAMPLE.

A global damage index, the total scattering cross-section, was computed to quantitatively evaluate the ASR damage extent using the collected ultrasonic data. The total scattering cross-section across the scanned area is computed by integrating scattered wave energy over the scanned area. For each block sample, three ultrasonic data sets were collected from different scan areas on the top surface of the block. The strain data measured from the reactive samples using embedded strain gauges nearby, although not precisely aligned with the scanned area, was compared with the global damage index. Comparison of the global damage index and the strain data for the embedded bars both indicate that the level of ASR damage progressed gradually for the reactive samples over time. The increasing trends of the two indicators show good agreement with each other. Conversely the global damage index values for the control sample do not show noticeable progress over time, indicating that ASR damage has not occurred in the control sample. Note that internal strain data were not collected for the control samples.

4. CONCLUSIONS

The following conclusions are drawn based on the presented material:

1) Distributed small-scale damage caused by ASR (ASR damage) scatter an incident wave and set up distinct incoherent

scattered wavefields that exhibit a broad range of wavenumbers;

2) The proposed frequency-wavenumber (f-k) domain wavefield data processing approach can extract incoherent multiple scattering content associated with ASR damage while at the same time suppressing that multiple scattering associated with a large-scale inhomogeneous base medium (i.e. aggregate networks); and

3) Extracting incoherent multiple scattering content enables location and characterization of ASR damage in concrete that also contains large-scale aggregates.

ACKNOWLEDGEMENTS

The work reported in this paper was performed with support from the Integrated Research Program by the DOE-Nuclear Energy Universities Program under Award number DE-NE0008266. The authors are also grateful to Chi-Luen Huang for his help with the field tests and to Dr. Steven Feldman and Dr. Fahim Sadek of the National Institute for Standards and Technology for providing access to the ASR test samples housed there and their measurement data.

REFERENCES

[1] Mehta, P.K., Monteiro, P.J.M. and Ebrary, I. "Concrete: microstructure, properties, and materials." 3rd Ed. (2006) McGraw Hill, New York.

[2] Johnson, S. "Degradation mechanisms and inspection techniques for concrete structures in dry storage systems for spent nuclear fuel." EPRI 3002005508 (2015), Palo Alto, CA.

[3] Aggelis, D.G. and Shiotani, T. "Experimental study of surface wave propagation in strongly heterogeneous media." *J. Acoust. Soc. Am.*, Vol. 122 (2007), EL151-157.

[4] Chekroun, M. Le Marrec, L., Abraham, O., Durand, O. and Villain, G. "Analysis of coherent surface wave dispersion and attenuation for non-destructive testing of concrete.", *Ultrasonics*, Vol. 49 (2009), pp. 743-751.